

Entropy Generation across Earth's Collisionless Bow Shock

G. K. Parks,^{1,*} E. Lee,² M. McCarthy,³ M. Goldstein,⁴ S. Y. Fu,⁵ J. B. Cao,⁶ P. Canu,⁷ N. Lin,¹ M. Wilber,¹
I. Dandouras,⁸ H. Réme,⁹ and A. Fazakerley¹⁰

¹Space Sciences Laboratory, University of California, Berkeley, California, USA

²School of Space Research, Kyung Hee University, Yongin, Korea

³Planetary and Space Sciences, University of Washington, Seattle, Washington, USA

⁴Goddard Space Flight Center, NASA, Greenbelt, Maryland, USA

⁵Institute for Space Physics and Applied Technology, Peking University, Beijing, China

⁶Space Science Institute, School of Aeronautics, Beihang University, Beijing, China

⁷Laboratory for Plasma Physics, Ecole Polytechnique, Paris, France

⁸University of Toulouse, UPS-OMP, IRAP, Toulouse, France

⁹CNRS, IRAP, BP44346, Toulouse cedex 4, France

¹⁰MSSL, University College London, London, England

(Received 7 October 2011; published 9 February 2012)

Earth's bow shock is a collisionless shock wave but entropy has never been directly measured across it. The plasma experiments on Cluster and Double Star measure 3D plasma distributions upstream and downstream of the bow shock allowing calculation of Boltzmann's entropy function H and his famous H theorem, $dH/dt \leq 0$. The collisionless Boltzmann (Vlasov) equation predicts that the total entropy does not change if the distribution function across the shock becomes nonthermal, but it allows changes in the entropy density. Here, we present the first direct measurements of entropy density changes across Earth's bow shock and show that the results generally support the model of the Vlasov analysis. These observations are a starting point for a more sophisticated analysis that includes 3D computer modeling of collisionless shocks with input from observed particles, waves, and turbulences.

DOI: 10.1103/PhysRevLett.108.061102

PACS numbers: 96.50.Fm, 52.35.Mw, 52.35.Tc, 94.30.vf

Introduction.—Collisionless shocks have been reported with supernova explosions, cosmic gamma ray bursts, and in our solar system from flares and coronal mass ejections that drive shocks and affect space weather. Corotating interaction regions in the free-flowing solar wind (SW) also form forward and reverse shock pairs, and Type II solar radio bursts are characterized by collisionless shocks that are the location of the radio emission. The best-known collisionless shock is Earth's bow shock. Even though the bow shock has been studied for nearly 50 years, many questions about thermalization and entropy generation processes remain poorly understood [1].

When the concept of a collisionless shock was first introduced [2], it received much attention from fusion researchers interested in heating plasma to high temperatures and astrophysicists seeking ways to accelerate particles to cosmic energies. Serious debates followed about what mechanisms could thermalize and produce entropy without collisions. However, these debates ended without a clear resolution of the theoretical issues when the super-Alfvénic solar wind was discovered [3]. The magnetic discontinuity in front of Earth (bow shock) was accepted as evidence of a collisionless shock.

The width of Earth's bow shock is about an ion Larmor radius, nearly 7 orders of magnitude smaller than the collision mean free path of the SW, which is about 1 AU. This discrepancy challenged theorists to look at collisionless shocks in new ways [4], but the physical mechanisms

of how the SW dissipates energy and generates entropy on scales of an ion Larmor radius remain unclear to this day.

Ludwig Boltzmann developed the concept of entropy in an atomic model of gases to resolve the mystery of why macroscopic systems are irreversible while the mechanics of individual particles in the systems are reversible. Boltzmann's entropy is $S = -k_B H$, where $H = \int f \ln f d^3v$. Here f is a one-particle distribution function, k_B is Boltzmann's constant, and the integration is performed over all velocities. Differentiation of H leads to the H theorem, $dH/dt = \int (1 + \ln f) \partial f / \partial t d^3v \leq 0$. The equality holds *only* if f is Maxwellian. The H function is always negative and given that a system can be in many different configurations, H will decrease to a minimum as f evolves to the most probable distribution corresponding to a state of maximum entropy.

For his analysis, Boltzmann considered a homogeneous gas at rest that changes in time. That situation is similar to the development seen by an instrument comoving within a magnetic flux tube of steady SW, as the flux tube crosses Earth's bow shock. However, the SW is nearly 2 orders of magnitude faster than spacecraft (SC) and SC move slowly with respect to the bow shock. Hence, for a steady SW, we interpret observed time variations as due to SC motion through spatial structures. Consistent with this viewpoint, we also interpret measurements along the SC track as a history of the plasma volume that traveled the same track.

Our plasma experiments on Cluster and Double Star [5,6] routinely measure 3D distributions $f(\mathbf{r}, \mathbf{v}, t)$ of the SW in regions upstream, downstream, and across Earth's bow shock. We have computed H and dH/dt across more than 20 relatively quiet shock crossings and have studied their behavior. Because particle instruments acquire $f(\mathbf{v})$ only at the spacecraft, and not throughout the unmeasured flux tube, we work with a normalized H function: $h = \sum p_i \ln p_i$, where $p_i = f_i \Delta^3 v_i / N$, N is particle number density, and i indexes the sampled phase space volume elements. This calculated h is proportional to entropy per particle (entropy density) at the spacecraft. The normalized $dh/dt = [h(t) - h(t - \Delta t)] / \Delta t$ is calculated from successive measurements, where Δt is the spin period of the spacecraft.

Here, we report for the first time that h changes systematically across the bow shock and that entropy production is intimately tied to mechanisms that produce the non-thermal distributions at the shock. These results, modeled with the Vlasov theory of how entropy flux should behave, show the agreement is quite good.

Entropy density across Earth's bow shock.—An example of how entropy behaves across the bow shock is illustrated from observations made on 1 February 2002 (Fig. 1). Magnetic field [7] measurements on the four Clusters showed the angle between the shock normal and the upstream magnetic field $\theta_{BN} \sim 82^\circ$ – 88° . The shock speed along its normal was $\sim 9 \text{ km s}^{-1}$ and the Alfvén Mach number was $M_A = (V/V_A) \sim 3.0$ – 3.5 . This is a supercritical perpendicular shock.

Cluster 1 was outbound and crossed the bow shock at $\sim 19:40:24 \text{ UT}$ shown by the magnetic field data [panel (a)]. The SW in the energy flux spectrogram plot appears as a red line centered around $\sim 600 \text{ eV}$ [panel (b), after 1940 UT]. The SW flow speed was $V_x \sim -320 \text{ km s}^{-1}$ and it slowed to $\sim 75 \text{ km s}^{-1}$ and deviated in y and z directions just before crossing the shock [panel (c)]. The plasma downstream of the shock (magnetosheath, MS) covers a broad energy range, $\sim 10 \text{ eV}$ to several keV [panel (b), <1940 UT] and the flow speed was $\sim 150 \text{ km s}^{-1}$.

The h function for the SW ions and electrons [panels (d), (e), black] shows h was -2.4 and -5.5 . These h values decrease across the magnetic ramp to -4.5 and -7.2 in the MS. The electron transition occurs more rapidly than the ions. The corresponding values of $s = -k_B h$ in the SW are $3.3 \times 10^{-16} \text{ ergs}^\circ \text{ K}^{-1}$ and $7.6 \times 10^{-16} \text{ ergs}^\circ \text{ K}^{-1}$ and in the MS $\sim 6.2 \times 10^{-16} \text{ ergs}^\circ \text{ K}^{-1}$ and $9.9 \times 10^{-16} \text{ ergs}^\circ \text{ K}^{-1}$. The increases of s across the shock are $\Delta s \sim 2.9 \times 10^{-16} \text{ ergs}^\circ \text{ K}^{-1}$ for ions and $2.3 \times 10^{-16} \text{ ergs}^\circ \text{ K}^{-1}$ for electrons. These entropy density changes are small and of the same order as entropy changes of isolated free expansion of an ideal gas when the volume changes by a factor of 2, $\Delta s \sim 0.95 \times 10^{-16} \text{ ergs}^\circ \text{ K}^{-1}$, and in ice at 0° C melting to water at the same temperature, $\Delta s \sim 3.3 \times 10^{-16} \text{ ergs}^\circ \text{ K}^{-1}$ (Δs per mole divided by Avogadro's number).

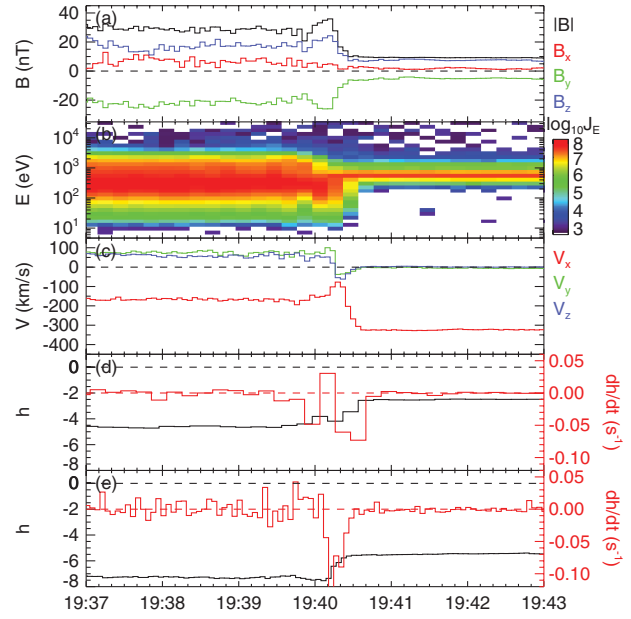


FIG. 1 (color). Bow shock crossing on 1 February 2002. These data come from a 3D electrostatic analyzer instrument that is an energy per charge detector and measures ions in the energy range $\sim 10 \text{ eV}$ to $\sim 35 \text{ keV}$ assuming all ions are H^+ . The ion data shown are 3 spin (12s) averages. Electrons are measured by a 3D instrument called PEACE (Plasma Electron And Current Experiment) and the data shown are one spin averages. PEACE is also an electrostatic analyzer and measured electrons in the energy range $\sim 5 \text{ eV}$ – 2.9 keV . Both instruments use position sensitive microchannel plates as detectors. The electron data shown are from SC2 (no 3D data on SC1) that was $\sim 600 \text{ km}$ from SC1. The bow shock crossing time has been shifted to coincide with SC1. From top to bottom: (a) B field and components in geocentric solar ecliptic coordinate system (x is positive toward the Sun, y is positive toward dusk and z is $\hat{x} \times \hat{y}$), (b) energy spectrogram of ions, (c) mean velocities computed from the 3D distribution functions, (d) h (black) and dh/dt (red) of ions, (e) h (black) and dh/dt (red) of electrons. (Because Cluster starts downstream of the shock and later moves upstream, it observes a reversed time history of a convected plasma volume. To compensate for this artifact of reference frame, the dh/dt traces have been inverted.)

These results are similar because the original energy per particle has an order of magnitude value of $k_B T$ and when the state change involves an amount of energy corresponding roughly to the original amount of energy, the associated entropy density change will be of the order of Boltzmann's constant. The bow shock results are simply stating that the compression ratio at Earth's bow shock is not some huge number (~ 3 on this day). If the ratio were really large as might happen in big astrophysical shocks (~ 1000 or so), then the entropy per particle is expected to be considerably larger than k_B .

The time variation of dh/dt is ~ 0 in the SW consistent with the SW distributions being nearly thermal [red, panels (e) and (f)]. Boltzmann assumed $\partial f / \partial t$ came from

collisions that redistributed the internal energy of the system but short-range collisions cannot be responsible for variations of f across the shock. dh/dt turns negative in the magnetic ramp to -0.07 s^{-1} for ions and -0.13 s^{-1} for electrons. The corresponding rate change across the shock is $\sim 0.1 \times 10^{-16} \text{ ergs}^\circ \text{ K}^{-1} \text{ s}^{-1}$ for ions and $\sim 0.18 \times 10^{-16} \text{ ergs}^\circ \text{ K}^{-1} \text{ s}^{-1}$ for electrons. The departure of dh/dt from 0 at the ramp indicates f is not Maxwellian there. Similar to the behavior of h , $dh/dt < 0$ for ions covers a broader region, extending from upstream SW to the downstream MS, whereas for the electrons it is more limited to the magnetic ramp region.

Note that dh/dt after crossing the shock turns *positive* before fluctuating about 0 in the MS. For this event, dh/dt for ions in the MS was not fluctuating much, but large $dh/dt > 0$ has been seen in many other bow shock crossings (not shown). The significance of $dh/dt > 0$ is not understood.

Distribution function.—To understand what could cause the entropy change, the distribution functions of the plasma in the vicinity of the shock have been examined (Fig. 2). The top two panels show ions and the bottom panels, electrons. Panels (a) and (b) are measured at 19:40:09, which is at the top of the magnetic ramp, and panels (c) and (d) measured at 19:40:21 are from the foot of the shock.

The multiple ion distributions (2D) observed on 1 February 2002 are consistent with the previous observations [8–12]. Ion distributions show three different populations: Panel (a) shows the solar wind beam and diffuse beam moving away from the shock and panel (b) shows the gyrating population. In panel (a), the solar wind ion beam can still be seen after going through the magnetic ramp indicating the SW distribution was not fully thermalized.

The electron distributions [Panels (e), (f)] are one-dimensional (1D) cuts of 3D distributions. Panel (e) is along V_{\parallel} and (f) along V_{\perp} . The colors represent different times, from the SW to MS (magenta, blue, green, red, and black). The changes of the electron distributions from the SW to MS are quite clearly seen in panel (e). The electron distributions normally show beamlike structure on the SW side and “flat” topped shaped distribution on the MS side [13,14]. The green line shows a small beamlike enhancement along V_{\parallel} , but for this particular pass, the 1D cuts were not well optimized to show the flow-associated beam as the B field was almost perpendicular to the SW.

Entropy flux.—The entropy change as a plasma element crosses the bow shock can be computed from the collisionless Boltzmann equation (Vlasov equation), $\partial f/\partial t + \mathbf{v} \cdot \partial f/\partial \mathbf{r} + \mathbf{a} \cdot \partial f/\partial \mathbf{v} = 0$. Multiply through with $\log f$ and obtain $\log f \partial f/\partial t + \log f \mathbf{v} \cdot \nabla f + \log f \mathbf{a} \cdot \nabla_v f = 0$ which can be rewritten as $\partial(f \log f)/\partial t + \nabla \cdot (\mathbf{v} f \log f) + \mathbf{a} \cdot \nabla_v (f \log f) - (\partial f/\partial t + \mathbf{v} \cdot \nabla f + \mathbf{a} \cdot \nabla_v f) = 0$ using the derivative of a product rule. The last term on the left side in the parentheses vanishes when f is a solution to the

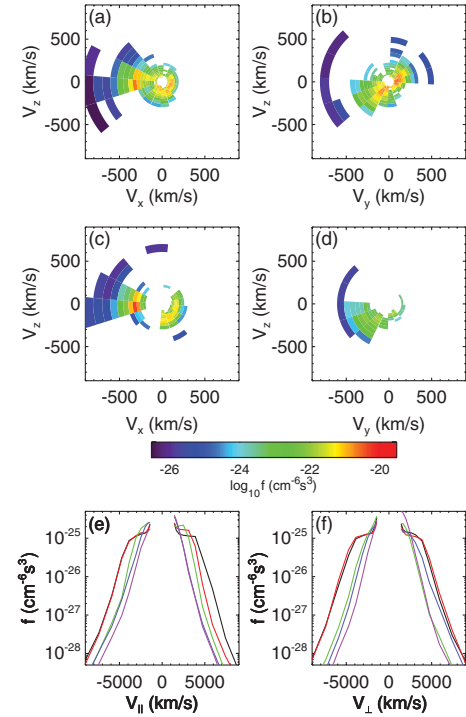


FIG. 2 (color). Top two rows: 2D cuts of the 3D velocity ion distributions measured by SC1 on 1 February 2001 displayed in the SC coordinates. V_x , V_y , and V_z are in the geocentric solar ecliptic coordinate system. Panels (a) and (b) show measurements made at the top of the magnetic ramp (19:40:09 UT). Panels (c) and (d) are measurements made at the foot of the shock (19:40:21 UT). Bottom row panels (e) and (f) are 1D cuts of the 3D electron distributions along velocities parallel and perpendicular to the direction of the magnetic field. The electron data come from SC2, which was $\sim 600 \text{ km}$ from SC1. The different colors represent different times: solar wind (magenta; 19:41:47 UT), magnetic ramp (blue 19:41:43 UT and green 19:41:39 UT), magnetosheath (red 19:41:35 UT and black 19:41:31 UT).

Vlasov equation. Then, integration over the velocity space yields,

$$\partial(ns)/\partial t + \nabla \cdot \int (-k_B \mathbf{v} f \log f) d\mathbf{v} = 0. \quad (1)$$

Here, $n = \int f d\mathbf{v}$ is the density, $ns = -k_B \int f \log f d\mathbf{v}$ is entropy flux, and k_B is Boltzmann’s constant. The integral of the last term in the bracket vanishes for \mathbf{a} equal to the Lorentz force. Equation (1) is the entropy conservation equation and the second term is the divergence of the entropy flux computed kinetically. Now change variables, $\mathbf{v} = \mathbf{U} + \mathbf{c}$, where \mathbf{U} is the velocity moment and define $f'(\mathbf{c}) = f(\mathbf{U} + \mathbf{c})$. Equation (1) can then be rewritten as

$$\partial(ns)/\partial t + \nabla \cdot (\mathbf{U} ns) = k_B \nabla \cdot \int \mathbf{c} f' \log f' d\mathbf{c}. \quad (2)$$

The right side of this equation vanishes for equilibrium processes in Vlasov plasmas corresponding to the adiabatic

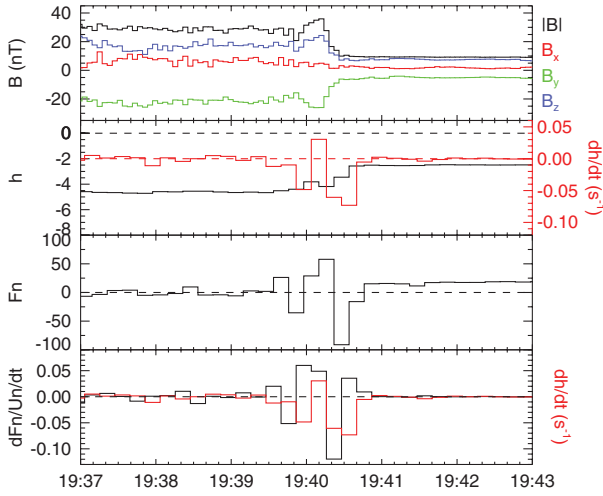


FIG. 3 (color). Shown are the magnetic field (top panel), h and dh/dt of ions [panel (2)], the kinetic function F_n [panel (3)], and the local change of per particle kinetic entropy flux, Eq. (3) [panel (4), black] superposed on dh/dt (red).

fluid case. However, at the bow shock, the distribution function is non-Maxwellian and the value of the integral is finite.

Assume, now, a steady state and 1D bow shock with x direction normal to the shock. Equation (2) then simplifies to $d(U_x n s - F_x)/dx = 0$; thus, $(U_x n s - F_x)$ is constant. Hence, $(U_{x1} n_1 s_1 - F_{x1}) = (U_{x2} n_2 s_2 - F_{x2})$, and using the mass conservation equation $U_1 n_1 = U_2 n_2$, we obtain

$$s_2 - s_1 = (F_{2x} - F_{1x})/U_1 n_1, \quad (3)$$

where $\mathbf{F} = k_B \int \mathbf{c} f' \log f' d\mathbf{c}$ and the subindices 1 and 2 are quantities measured in the upstream and downstream regions. U_1 is the flow in the normal direction, which is determined from the minimum variance analysis. For processes that produce non-Maxwellian distribution functions, the right side of Eq. (3) gives the amount of per particle entropy change in this simplified Vlasov model.

The left side $(s_2 - s_1)$ has already been computed (Fig. 1). Figure 3 shows the new terms on the right of Eq. (3) for ions (No 3D electron data on SC1). The data here were obtained when the SW flow was not varying significantly during the time it took to measure both sides of the shock, and we assume that we are equivalently looking at the same flux tube of plasma but at earlier and later times. The fact that the behavior of dh/dt (red) and $(F_2 - F_1)/U_1 n_1$ (black) is “similar” is no proof of the Vlasov theory; rather, it indicates our results generally support the plasma model of the Vlasov analysis.

Summary and discussion.—We measured entropy density that increased across Earth’s bow shock. Our observations are consistent with the Vlasov model of entropy that predicts entropy density can be locally generated when the distribution function is non-Maxwellian.

This analysis included only the distribution function of charged particles. However, complex electromagnetic waves permeate the shock region [15] and entropy generation theory must include the electromagnetic field. Unfortunately, a self-consistent theory including waves and particles is currently not available. Further data analysis combined with computer modeling with measured shock parameters would be invaluable in revealing new clues about energy dissipation and entropy generation in collisionless plasmas observed throughout the universe.

The research at UC Berkeley is funded by NASA Grant No. NNX07AP96G and at Kyung Hee University by the WCU program through NRF funded by MEST of Korea (Grant No. R31-10016).

*parks@ssl.berkeley.edu

- [1] N. A. Krall, *Adv. Space Res.* **20**, 715 (1997).
- [2] T. Gold, *Gas Dynamics of Cosmic Clouds*, IAU Symposium Vol. 2 (North Holland Publishing, Amsterdam, 1955).
- [3] N. F. Ness, C. S. Scarce, and J. B. Seek, *J. Geophys. Res.* **69**, 3531 (1964).
- [4] D. A. Tidman and N. A. Krall, *Shock Waves in Collisionless Plasmas* (Wiley/Interscience, New York, 1971).
- [5] H. Réme *et al.*, *Ann. Geophys.* **19**, 1303 (2001).
- [6] A. D. Johnstone *et al.*, *Space Sci. Rev.* **79**, 351 (1997).
- [7] A. Balogh *et al.*, *Ann. Geophys.* **19**, 1207 (2001).
- [8] M. Montgomery, J. R. Asbridge, and S. J. Bame, *J. Geophys. Res.* **75**, 1217 (1970).
- [9] G. Paschmann, N. Sckopke, S. J. Bame, and J. T. Gosling, *Geophys. Res. Lett.* **9**, 881 (1982).
- [10] N. Sckopke, G. Paschmann, S. Bame, J. Gosling, and C. Russell, *J. Geophys. Res.* **88**, 6121 (1983).
- [11] N. Sckopke, G. Paschmann, A. Brinca, C. Carlson, and H. Lühr, *J. Geophys. Res.* **95**, 6337 (1990).
- [12] N. Sckopke, *Adv. Space Res.* **15**, 261 (1995).
- [13] W. C. Feldman *et al.*, *J. Geophys. Res.* **88**, 96 (1983).
- [14] J. Scudder, *Adv. Space Res.* **15**, 181 (1995).
- [15] D. A. Gurnett, in *Collisionless Shocks in the Heliosphere: Reviews of Current Research*, edited by B. T. Tsurutani and R. G. Stone, Geophysical Monograph Vol. 35 (American Geophysical Union, Washington, D. C., 1985), p. 207.